Simultaneous adjustment of balance maintenance and velocity tracking for a two-wheeled self-balancing vehicle

Journal:	*Part C: Journal of Mechanical Engineering Science*
Manuscript ID	JMES-23-1504.R1
Manuscript Type:	Original Research Article
Date Submitted by the Author:	n/a
Complete List of Authors:	Ghahremani, Azadeh; University of Bergamo Department of Engineering and Applied Sciences, Department of Engineering and Applied Sciences University of Bergamo Righettini, Paolo; University of Bergamo Department of Engineering and Applied Sciences Strada, Roberto; University of Bergamo Department of Engineering and Applied Sciences
Keywords:	Two-wheeled self-balanced vehicle, Sliding Mode Control, Feadback linearization, PID control, LQR method, Stabilization, Tracking, Adams-Matlab co-simulations
Abstract:	The purpose of this research is the development a method for simultaneously adjusting the velocity tracking control and the inclination angle stabilization using control techniques for a two-wheeled self-balancing vehicle. In this study, the mathematical dynamic model of the vehicle is derived using the Lagrange method, under the assumptions of pure rolling and no-slip conditions. Along with the mathematical descriptions, a multibody virtual prototype featuring advanced tire-ground interaction modelling has been developed using the MSC Adams software suite. Several classical and modern control strategies are investigated and compared to implement the method. These include Sliding Mode Control (SMC), Proportional Integral Derivative (PID), Feedback Linearization, and Linear Quadratic Regulator Control (LQR) for the under-actuated and unstable subsystem that accounts for the pitch and longitudinal motions. The capabilities of these control strategies are verified and compared not only through Matlab simulation but also using Adams-Matlab co-simulation of the controller and the plant. Although every control technique has its advantages and limitations, the extensive simulation activities conducted for this study suggest that the SMC controller offers superior performances in keeping the system balanced and providing good velocity-tracking responses. Moreover, a Lyapunov-based analysis is used to prove that the sliding mode control achieves finite time convergence to a stable sliding surface. These advantages are counterbalanced by the complexity and the large number of parameters belonging to the designed SMC laws, the scheduling of which can be difficult to implement. For the comparison results feedback linearization method, is presented as an alternative. Through the Jacobian linearization approach the mathematical model of the system is linearized, allowing to design linear quadratic regulation, which are deployed to treat the balancing, steering, and velocity tracking tasks. The performance and robustness of each controller are evaluated and compared through several driving scenarios both in pure-Matlab and Matlab-Adams co-simulations.

Simultaneous adjustment of balance maintenance and velocity tracking for a two-wheeled self-balancing vehicle

Azadeh Ghahremani[1*], Paolo Righettini[1], Roberto Strada[1]

[1] Department of Engineering and Applied Sciences, University of Bergamo, Italy

*Corresponding author: E-mail: azadeh.ghahremani@gmail.com

Abstract

The purpose of this research is the development a method for simultaneously adjusting the velocity tracking control and the inclination angle stabilization using control techniques for a two-wheeled self-balancing vehicle. The control tasks involve balancing the vehicle around its unstable equilibrium configuration along with steering and velocity tracking. In this study, the mathematical dynamic model of the vehicle is derived using the Lagrange method, under the assumptions of pure rolling and no-slip conditions which are expressed through nonholonomic constraint equations. Along with the mathematical descriptions, a multibody virtual prototype featuring advanced tire-ground interaction modelling has been developed using the MSC Adams software suite. Several classical and modern control strategies are investigated and compared to implement the method. These include Sliding Mode Control (SMC), Proportional Integral Derivative (PID), Feedback Linearization (FL), and Linear Quadratic Regulator Control (LQR) for the under-actuated and unstable subsystem that accounts for the pitch and longitudinal motions. The capabilities of these control strategies are verified and compared not only through Matlab simulation but also using Adams-Matlab co-simulation of the controller and the plant. Although every control technique has its advantages and limitations, the extensive simulation activities conducted for this study suggest that the SMC controller offers superior performances in keeping the system balanced and providing good velocity-tracking responses. Moreover, a Lyapunov-based analysis is used to prove that the sliding mode control achieves finite time convergence to a stable sliding surface. These advantages are counterbalanced by the complexity and the large number of parameters belonging to the designed SMC laws, the scheduling of which can be difficult to implement. For the comparison results another non-linear control strategy, i.e. the feedback linearization method, is presented as an alternative. Through the Jacobian linearization approach the mathematical model of the system is linearized, allowing the use of control techniques such as linear quadratic regulation, which are deployed to treat the balancing, steering, and velocity tracking tasks. Finally, the empirical tuning of a PID controller is also demonstrated. The performance and robustness of each controller are evaluated and compared through several driving scenarios both in pure- Matlab and Adams-Matlab co-simulations.

Keywords: Two-wheeled self-balanced vehicle; Matlab-Adams co-simulations; Sliding Mode Control; Feadback linearization; PID control; LQR method, Stabilization, Tracking

1. Introduction

As contemporary urbanization reaches unprecedented scale and intensity, personal transportation is a topic of particular interest, especially in relation to the combined needs of low emission, high maneuverability, and reduced parking space occupation. A Two-Wheeled Self-Balancing Vehicle (TWSBV) is defined as a small size vehicle, which composed of an unbalanced intermediate chassis, a steering rod, and two wheels mounted on each side of the chassis frame which is equipped with electric actuators and sensors. The Segway is a commercial example of a two-wheeled self-balancing vehicle. The forward or backward motion of the TWSBV can be obtained by the operator through the small perturbation of the angular position of the rod (the rod is rigidly attached to the chassis; therefore the tilt angle of the rod coincides with the tilt angle of the chassis). Moreover in order to turn the TWSBV or to travel in an arc shape, the driver has to shift his or her body weight on the left or on the right foot; in other words the driver signals the turning direction by a

corresponding shift of their center of gravity. This force distribution change can be sensed by appropriately configured transducers. The peculiar characteristics of the TWSBV include inherent instability and under-actuated and highly nonlinear coupled dynamics, which are featured in many other important practical applications like building stabilization under action of earthquakes and which make the system especially challenging from a control perspective.

Generally, studies concerning TWSBV can be classified into two main fields: modelling on one hand and control on the other. Moreover, the studies concerning the TWSBV can be classified according to the role envisioned by the researchers for the device itself, which can serve either as a personal transportation vehicle or as an autonomous or remotely controlled mobile robot. Some studies are inspired by the inverted pendulum system and involve the creation of small-size robots, while other publications are more focused on the design and construction of a full-scale TWSBV to transport passengers or goods. Some research as mentioned above has been focused on modelling issues; in [1, 2] comprehensive information on the modelling of the TWSBV is provided. Typical TWSBV mathematical model development is performed by Euler-Lagrange analysis [3]; however, Newton modelling [4] has been also well studied, while Kane's method in [1] has been investigated. Within the TWSBV system, the number of actuators is less than the number of degrees of freedom. Although controlling an under-actuated system is more challenging compared to fully actuated systems, it can also bring advantages such as reduced bulk and mechanical complexity. As such, it deserves more investigation in theory and practice. The two-wheeled self-balancing vehicle has been subjected to various control techniques. In [5] partial feedback linearization is designed to control the two-wheeled inverted pendulum system. In [6] Adaptive control is designed using a network neural function RBF and an SMC for the two wheeled self-balanced robot. In [7] the sliding mode control is used for the stabilization of the robot and the disturbance rejection. In [8] the authors have validated the robustness of the SMC and LQR controllers in the presence of matched uncertainties and input disturbance. In [9] concerns optimal control of the linear motion, tilt motion, and yaw motion of a two-wheeled self-balancing robot in the presence of disturbance. The hierarchical sliding mode control with perturbation estimation technique has been designed on a two-wheeled inverted pendulum system for the two tasks of balancing and velocity tracking [10]. In [11] the authors verified that the settling time of a sliding mode controller compares favorably to PID, state feedback, and LQR controllers. The effects of uncertain rolling resistance between the wheel and surface have been furthermore investigated in [12]. The Genetic optimization algorithm has been applied in [13] to find the best PID gain values for fastest stability. The majority of the literature concentrated on developing control algorithms to keep the vehicle balanced and on checking the performance of the system, typically using the Matlab-Simulink software suite. Commonly the mathematical descriptions of the TWSBV are driven for simplicity by the assumption of pure rolling, no-slip conditions which are expressed through nonholonomic constraint equations. However, there are few and rare studies that considered joint and ground frictions [14,15]. It should be noted that to generate traction forces at the contact point between the wheel and the surface micro-slipping is necessary. Due to the Industrial applications benefit with regard to introducing controller that can guarantee the performance of system in real-world, our study has been carried out. Since the structure of the proposed control algorithm is based on the simplification of mathematical model to keep the controller design easy [16]. Hence, to clarify the effect of nonholonomic constraint on performance of system, before transitioning it to real-world applications [17]. It is necessary to be verified the performance of controller for both models with slippery road case and a with assumption of pure rolling, no-slip.

Therefore, in this paper, a multibody virtual prototype featuring advanced tire-ground interaction modelling has been developed using the MSC Adams software suite. MSC Adams is a virtual prototyping simulation software dedicated to multi-body dynamics which allows the user to create highly detailed models of engineering mechanical systems. Moreover, the availability of an interface between the multi-body physics simulation and the Matlab-Simulink software enables the validation of control systems typically designed using simplified representations of the actual plant on a more realistic virtual model. With respect to the control of the TWSBV, the most challenging task is achieving satisfactory results for longitudinal motion control performance as well as maintaining the upright position of the vehicle body, both in pure-Matlab and in an Adams-Matlab co-simulation. In article [1], it is shown that the control

strategy therein proposed can successfully stabilize the adopted mathematical model of the TWSBV. However, the verification of the underlying modelling assumptions is lacking, making it difficult to predict the controller performance when applied to an actual system. On the other hand, the use of Adams to simulate the mechanical dynamics of the vehicle and to verify the controller performance has convinced us of the robustness of the proposed controllers. We would like to highlight the fact that the full power of the Adams software can be deployed to account for physical effects such as slipping conditions and road-tire interaction forces that are usually left unmodeled in the analytic representation of the vehicle used for control purposes. As such, the Adams-Matlab co-simulation represents a highly useful intermediate step between the design of the controller and its experimental validation on a physical prototype. The main contributions of this study pertain therefore to two aspects: on the one hand, proposing the α method for adjusting the velocity tracking control and the linclination angle stabilization using control techniques based on the ideal case (characterized by the assumption of no-slip conditions between the road and the wheel) to the mathematical model of the plant, as implemented directly in Matlab; on the other hand to confirm and compare the robustness and effectiveness of different control algorithms a Adams-Matlab co-simulation is implemented. The content of this study can be organized into three main sections: in section 2 methodologies for deriving the equations of motion of the TWSBV are presented. In section 3 the multibody Adams model is described along with the creation of an interface with the Matlab-Simulink environment. The control strategies presented in this work are subsequently detailed in section 4. The study is concluded in section 5 with a summary of completed work. The future research is described in section 6.

2. Mathematical Modeling

The mathematical model of the two-wheeled self-balancing vehicle is needed not only for simulation purposes, but also to guide the design of the mechanical structure, to choose an appropriate actuation system, and for the synthesis of the closed loop regulator of any physical prototype. Given such a foundational role played by modelling, a physics-based approach has been adopted to develop from first principles a concise set of equations that describes the dynamics of the system. The Lagrange methodology is perhaps more familiar and widely described in the literature [1, 2, 17]. Fig. 1 shows the schematic diagram of the TWSBV, with the assumption of pure rolling and no-slip conditions (slip in tires is ignored). It is composed of an unbalanced intermediate chassis, a steering rod, and two wheels mounted on each side.

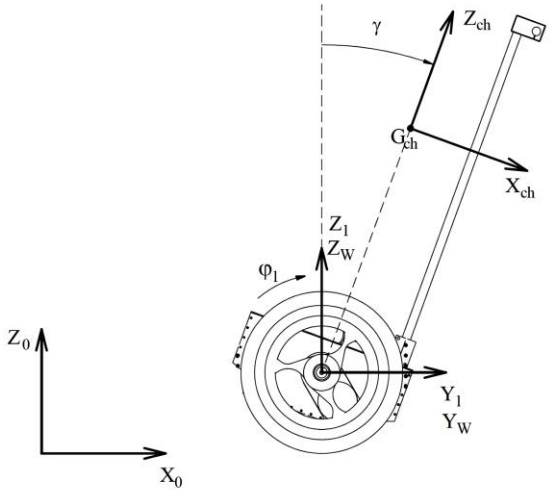

Fig. 1: Schematic diagram of the TWSBV and denotations.

A description of the relevant parameters has been provided in Table. 1 and Table 2.

Table 1. The parameters and variables of the TWSBV

Notation	Definition
Torques of left and right wheels	τ_1, τ_2
Rotational angles of the left and right wheels	φ_1, φ_2
The position coordinates of the system in X–Y plane	x, y
The inclination angle of TWSBV	γ
Yaw angle of TWSBV	θ

Table 2: The parameters and variables of the TWSBV

Definition	Notation	Value	Unit
Mass of chassis(mass of driver is included)	m_{ch}	120	kg
Mass of the wheel	m_w	3	kg
Inertia moment of the chassis about the $Y_{3_{ch}}$	$I_{yy_{ch}}$	15.7	kg. m^2
Inertia moment of the chassis about the $X_{3_{ch}}$	$I_{xx_{ch}}$	36	kg. m^2
Inertia moment of the chassis about the $Z_{3_{ch}}$	$I_{zz_{ch}}$	37.5	kg. m^2
Inertia moment of the chassis about the $X_{3_{ch}}$	I_{w1}	0.048	kg. m^2
Inertia moment of the chassis about the $Y_{3_{ch}}$	I_{w2}	0.027	kg. m^2
Gravity Acceleration	g	9.81	m^{2}s^{-1}
The radius of the wheel	r_w	0.2	m
Half of the distance between the wheels	l	0.3	m
Distance from the middle point between two wheels to the centre of gravity of the chassis	h	0.3	m

The chassis of the TWSBV has three degrees of freedom, namely the longitudinal motion and the rotations around the x-axis and the y-axis. In order to describe the full dynamics of the three degrees of freedom, the following generalized coordinates $[x, y, \theta, \gamma, \varphi_1, \varphi_2]$ are introduced. Since ideal control of this type of physically unstable vehicle is desired, the first step is modelling the dynamic behaviour of the system. Nevertheless, the dynamic analysis of TWSBV is challenging, because of the dynamic behaviour of the two wheels which are subjected to nonholonomic constraints; as a result, two types of equations govern the motion dynamics of TWSBV. These include equations of motion of the wheels under the condition of pure rolling without slipping, and the equations describing the dynamic behaviour of the whole system. Under the adopted assumption of sufficient friction between the wheel and the ground, the instantaneous velocity of the point of contact between the two is equal to zero at all times. It is important to note that the centre of mass represented in Fig.1 takes into account also the driver (which is not shown in the schematics) but the mass has been presented in Table 2.

Based on the assumption of pure rolling and no-slipping, the Lagrange method is employed to obtain the general system dynamics, as described by equations (1-3), [1].

$$(3m_w + m_{ch})\dot{u} + h\, m_{ch}(\ddot{\gamma}\cos\gamma - \dot{\gamma}^2 \sin\gamma - \dot{\theta}^2 \sin\gamma) = \frac{1}{r_w}(\tau_1 + \tau_2) \tag{1}$$

$$\left(2(m_w l^2 + l_{cw}) + I_{xx}\sin^2\gamma + m_{ch}h^2\sin^2\gamma + \mathrm{I_{zz_{ch}}}\cos^2\gamma + m_w l^2\right)\ddot{\theta} + (m_{ch}h^2 + \mathrm{I_{xxch}} - I_{zzch}\sin 2\gamma\,\dot{\theta}\dot{\gamma} + m_{ch}h\sin\gamma\dot{\theta}u = \frac{1}{\mathrm{r_w}}(\tau_1 + \tau_2) \tag{2}$$

$$(I_{yy_{ch}} + m_{chh}^2)\ddot{\gamma} + m_{chh}\cos\gamma\, \dot{u}\left(\frac{1}{2}(I_{xx_{ch}} - m_{ch}h^2 - I_{zz_{ch}})\sin 2\gamma\,\dot{\theta}^2\right) - m_{ch}gh\sin\gamma = -(\tau_1 + \tau_2) \tag{3}$$

In addition, in order to facilitate the definition of the system model and the design of the controller, we define $\tau_1 + \tau_2 = \tau_v$ and $\tau_1 - \tau_2 = \tau_w$. For simplification of the system analysis, new symbolic functions $\Lambda_u, \Psi_u, X_u, \Phi_u, \Lambda_\gamma, \Psi_\gamma, X_\gamma, \Phi_\gamma, \Lambda_\theta, \Psi_\theta$ and X_θ are introduced, which are given in Appendix 1. Thus the final equations of motion of the TWSBV can be expressed by substituting the expressions above in Eqs. (7-9), yielding:

$$\dot{u} = \Lambda_u\dot{\theta}^2 + \Psi_u\dot{\gamma}^2 + X_u\tau_v + \Phi_u g \tag{4}$$

$$\ddot{\gamma} = \Lambda_\gamma\dot{\theta}^2 + \Psi_\gamma\dot{\gamma}^2 + X_\gamma\tau_v + \Phi_\gamma g \tag{5}$$

$$\ddot{\theta} = \Lambda_\theta \dot{\theta}^2 u + \Psi_\theta \dot{\theta}\dot{\gamma} + X_\theta \tau_w \quad (6)$$

Furthermore, the overall dynamic system is separated into two decoupled algebraically independent subsystems: one is the longitudinal motion subsystem while the other is the steering subsystem. The steering subsystem is a single-input, single-output (SISO) system, that has a simple dynamic description, while the longitudinal motion subsystem is a single-input, multi-output (SIMO) system, which has two output variables to be controlled, namely pitch angle γ and longitudinal velocity u using a single input τ_v to be determined by the control system.

3. Multibody Virtual Model

The configuration of the vehicle is shown in Fig. 2 and Fig. 3. In particular, Fig. 2 represents the 3D CAD model of the vehicle, while Fig. 3 shows an inner view of the chassis. The vehicle is composed of the chassis, two DC electric motors to drive the wheels, two gearboxes connected on one hand to the motors' shafts and on the other to the driving pulley of a timing belt transmission that proves a further speed reduction to the wheels and the tires. The motors are powered by batteries. The internal layout of the chassis (Fig. 3) is therefore as follows: motors (a), gearboxes (b), and timing belts.

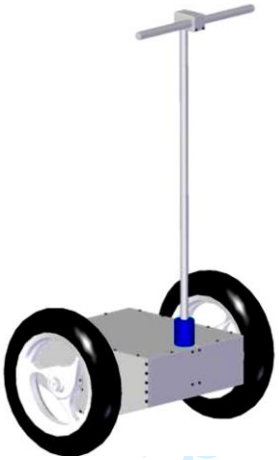

Fig. 2: 3D Model of the TWSBV system.

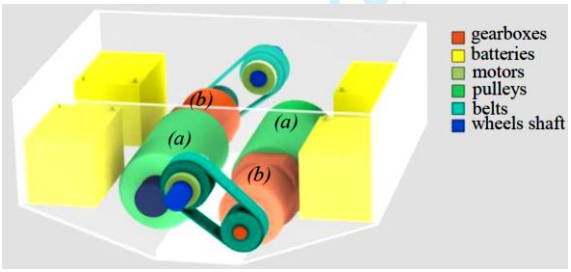

Fig. 3: Chassis' Internal Layout.

3.1 Adams Model

The model used for controller design doesn't take into account some characteristics of the real system, like the presence of tires between the wheels and the ground which makes the ideal no-slipping hypothesis no more valid. Hence, to better approximate the real behaviour of the system, a more realistic dynamic model, which includes also the tires, has been developed with MSC Adams, as shown in Fig. 4. The tires have been widely discussed by Pacejka [18]. The tires model used in this paper is the 5.2.1 Model 16, because of its simplicity and a small set of parameters; since the simulation are performed on flat ground, combined effects are negligible and the camber angle is absent. The main parameters of the tire are the vertical stiffness k_Z, which slightly increases for small deformations, vertical damping c_Z, and longitudinal friction μ.

Fig. 4: Adams Model.

The latter parameter is defined as a function of the slip speed v_{sx}. Fig. 5 shows the tire slip quantities, while Fig. 6 shows the shape of the function $\mu(v_{sx})$. According to Pacejka's model 5.2.1, longitudinal force F_x and lateral force F_y are expressed by the following equations:

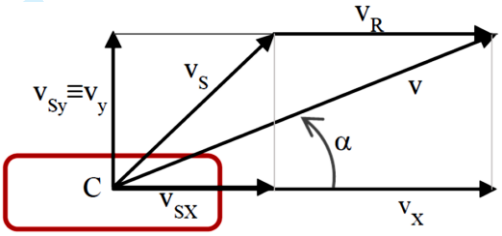

Fig. 5: Tire Slip Quantities 16

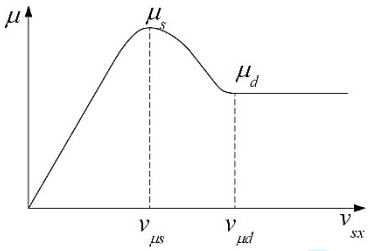

Fig. 6: Friction Coefficient μ vs. Local Speed Velocity 16

$$F_x = \mu F_z \tag{7}$$

$$F_y = -[\mu_{stat} F_z(1 - e^{k_\alpha|^\alpha|})sign(\alpha)] \tag{8}$$

$$F_z = F_{stiff} - F_{damp} \tag{9}$$

Where F_z depends on tire deformation d and deformation speed v_z as follows:

$$F_{stiff} = k_z d^{(\sigma)} \tag{10}$$

$$F_{damp} = c_z v_z \tag{11}$$

The tire slip speed depends on the wheel's longitudinal speed v_x and the wheel's rolling speed ΩR_1:

$$v_{sx} = v_x - \Omega R_1 \tag{12}$$

Where Ω and R_1 are the angular speed and the radius of the wheel, respectively. The rolling resistance moment is calculated as follows:

$$M_y = f_v F_z R_1 \tag{13}$$

The tire's parameters have been properly selected and integrated within the MSC Adams model. Their values are summarized in Table 3. As far as the other vehicle's components are concerned, motors have been

modelled as massive rotors revolving with respect to the stator, fixed to the chassis; moreover, the motors are modelled as ideal torque generators and the control torque (action between rotor and stator) is applied according to the different control strategies adopted, as subsequently described. Gearboxes between motors and wheels are modelled through their kinematic relationship between input and output speed. Similarly, the timing belts are kinematically simulated, utilizing the coupler joint of Adams. Moreover, in order to measure the state of the system, sensors are used in Adams that match the transducers placed on the real system.

Table 3: Tire parameters

Definition	Notation	Value	Unit
Vertical stiffness	k_z	206	N/mm
Vertical stiffness exponent	θ	1.1	
Vertical damping	c_z	2.06	Ns/mm
Lateral stiffness	k_y	50	N/mm
Cornering stiffness coefficient	k_α	50	N/deg
Static friction coefficient	μ_s	0.95	
Dynamic friction coefficient	μ_d	0.75	
The velocity of the static friction coefficient	v_{μ_s}	3000	mm/s
The velocity of the dynamic friction coefficient	v_{μ_d}	6000	
Rolling resistance coefficient	f_v	0.01	mm/s

The Adams software can be used not only for the automatic formulation of equations accurately describing linear and nonlinear mechanical dynamics but also to embed such a model within the Matlab-Simulink environment. Adams/Matlab co-simulation of the controller prototyped in Simulink and of the plant implemented in Adams is thus achieved.

In this subsection, the Adams-Matlab co-simulation environment which combines Adams and Matlab-Simulink is employed to validate the proposed control strategies. The virtual prototype of the TWSBV is built in the Adams environment and subsequently imported into Matlab's Simulink. As a result, the inputs of the Adams virtual prototype are generated from the output of the proposed controller. Moreover, the state variables of the Adams virtual model are fed back to the controller deployed to regulate them. Fig. 7 shows the Adams-Matlab co-simulation block diagram of TWSBV which contains two inputs and six measurable state variables. Moreover, the general block diagram depicting a general control system acting on the multibody model can be seen in Fig. 8. In the following the Adams-Matlab co-simulation results are utilized for the verification and improvement of the examined controllers.

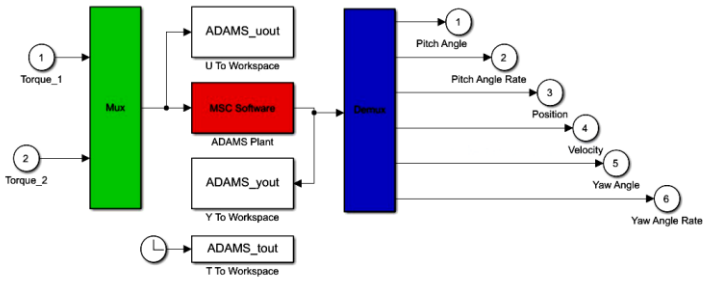

Fig. 7: Adams-Matlab co-simulation.

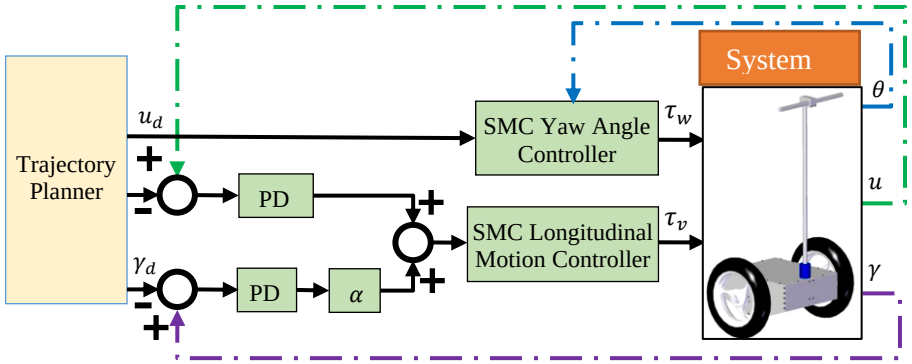

Fig. 8: General control structure for longitudinal velocity, tilt angle and yaw angle control.

4. Control System Design

The purpose of this section is to present a model-based approach to the design of the control architectures for the TWSBV. The main assets that have been leveraged to design each controller are the mathematical model implemented in Matlab and the more detailed prototype developed in Adams. In particular, the general strategy is to tune the controller parameters using the lightweight Matlab simulation; each tuned controller was then used within the Adams-Matlab co-simulation. As might be expected, given the discrepancies between the two models, the Adams-Matlab co-simulations tend to highlight a deterioration of the performance of the controller if compared with the results provided by the pure-Matlab analysis. In particular, in all cases, the use of an unmodified controller leads to failure in the stabilization task. However, a key parameter, shared by all controller families, was identified and acted upon in order to restore the self-balancing capabilities of the vehicle without the need to re-tune all the gains of the control system. This parameter, which will be denoted as α, is the quantity used to treat the underactuated nature of the longitudinal subsystem. As will be shown in the following sections, α is responsible, in various forms, for the definition of one controllable output which is a function of both pitch and longitudinal velocity. In particular, α can be manipulated to prioritize the balancing task. The modified controller still suffers from a performance loss in its tracking capabilities but regains the ability to hold the TWSBV around the unstable equilibrium configuration. The advantages and disadvantages of controllers in the scope of this work also are highlighted.

4.1 Reference velocity Trajectory generation

The above discussion dealt with TWSBV modelling; however, the definition of the longitudinal reference velocity has not until now been considered. On the other hand, it is well known that the acceleration and deceleration capabilities of the vehicle contribute to determine its handling and safety characteristics. Hence the velocity references selected for evaluation purposes within the scope of this work feature acceleration and deceleration periods, separated by a phase where a stationary cruise velocity is held. Accordingly, the motion profile can be entirely characterized by the following parameters:

– initial and final velocity u_0, u_f;
– maximal velocity u_m;
– acceleration and deceleration time intervals;
– stationary velocity time interval.

As shown in Fig. 9, the resulting reference velocity trajectory is characterized by a trapezoidal profile. Analytically such a velocity function can be specified as shown below:

$$u_d(t) = \begin{cases} u_0 + (u_m - u_0)\left(\dfrac{t}{t_a - t_0}\right) & if\ t \in [t_0, t_a) \\ u_m & if\ t \in [t_a, t_b) \\ u_m - (u_m - u_f)\left(\dfrac{t - t_b}{t_f - t_b}\right) & if\ t \in [t_b, t_f) \end{cases} \quad (14)$$

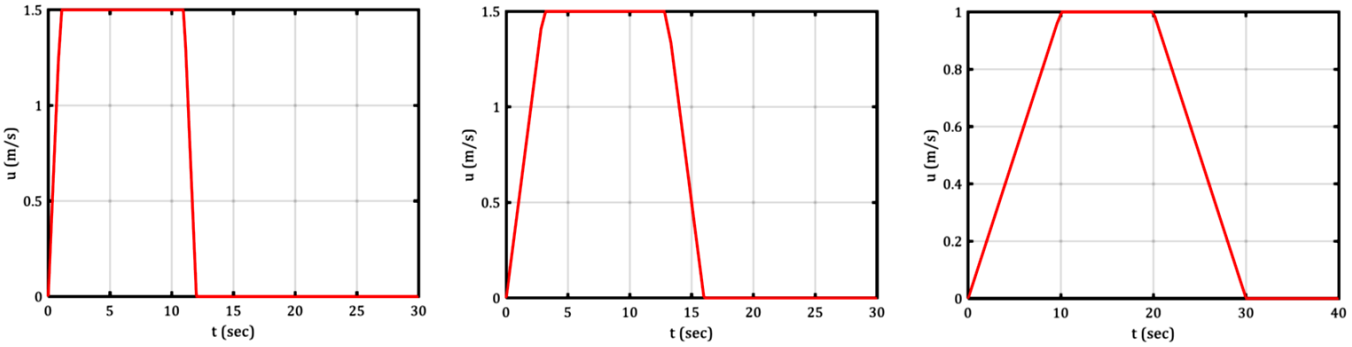

Fig. 9: Velocity Reference Profiles.

Different values for parameters of Eq. 17 are considered, in Table 4.

Table 4: The Motion Profile Parameters

Motion cases	t_0	t_a	t_b	t_f	u_0	u_m	u_f
motion case a	0	1	11	12	0	1.5	0
motion case b	0	3	13	16	0	1.5	0
motion case c	0	10	20	30	0	1	0

4.2 Sliding Mode Controller

The controller designed using the SMC method [19] is particularly appealing due to its ability to deal with nonlinear systems and disturbances. Sliding mode control principles have been successfully applied in a wide range of problems, which for example include state-space systems, chemical processes, robotics, and mechatronic systems. The main core of sliding mode control is related to the satisfactory design of the function which expresses the sliding surface for the controlled variables. In other words, the idea behind SMC is to define a surface along which the process can slide to its desired set point [20]. Therefore, the first step in designing SMC is the definition of the sliding surface $s(t)$. The sliding surface is chosen to represent the desired behavior for the selected sliding variables; in our case, such behavior features the convergence of the tilt angle to zero and the tracking of the longitudinal velocity set point.

Therefore, we need two sliding mode surfaces for the two sliding variables γ, u to design the control law for τ_v, which represents the sum of the torques applied to the wheels. The sliding surface $s(t)$ has been chosen in this study as the differential equation governing the tracking error which can generally be defined, as follows:

$$s(t) = \left(\frac{d}{dt} + c\right)^n e(t) \tag{15}$$

In Eq. 18, e(t) is the tracking error i.e. the difference between the set point and output measurement; c is a tuning parameter, which helps to adjust the convergence rate. This term is selected by the designer and determines the performance of the system. The constant n is the system order. In order to define control errors, we can select state variables [x, u, γ, $\dot{\gamma}$]. The control errors are then defined as: $e_1 = x - x_d$, $e_2 = u - u_d$, $e_3 = \gamma - \gamma_d$, $e_4 = \dot{\gamma} - \dot{\gamma}_d$, where x_d is the desired longitudinal position, u_d represents the desired longitudinal velocity, while γ_d and $\dot{\gamma}_d$, the desired inclination angle and angular velocity, which can be set to zero. The system error dynamics can be expressed as

$$\dot{e}_1 = e_2 \tag{16}$$

$$\dot{e}_2 = \Lambda_u \dot{\theta}^2 + \Psi_u \dot{\gamma}^2 + X_u \tau_v + \Phi_u g - u_d \tag{17}$$

$$\dot{e}_3 = e_4 \tag{18}$$

$$\dot{e}_4 = \Lambda_\gamma \dot{\theta}^2 + \Psi_\gamma \dot{\gamma}^2 + X_\gamma \tau_v + \Phi_\gamma g - \dot{\gamma}_d \tag{19}$$

The objective of the control is to ensure the convergence of the controlled variables to the desired values. Hence, for controlling two variables, the inclination angle and the longitudinal velocity, two sliding surfaces should be designed. For the intended purposes, two sliding surfaces are described by equations (20-21).

$$s_1 = \dot{e}_1 + c_1 e_1 \tag{20}$$

$$s_2 = \dot{e}_3 + c_2 e_3 \tag{21}$$

Fundamentally as mentioned before, two types of control tasks should be designed to maintain the inclination angle (balancing) and track the desired longitudinal velocity at the same time. Since the longitudinal motion subsystem has a SIMO structure with one input and two outputs, a third sliding surface is needed to fulfil both control aims. In order to achieve this goal, the constant positive integer value α has been defined to give priority to the balancing as follows:

$$S = s_1 + \alpha s_2, \quad \alpha > 0 \tag{22}$$

In order to maintain S at a constant value, $dS(t)/dt = 0$

$$\dot{S} = \dot{s}_1 + \alpha \dot{s}_2 \tag{23}$$

Next, substituting from Eqs. (17, 19) into (23) the yields:

$$\dot{S} = \dot{e}_2 + c_1 e_2 + \alpha(\dot{e}_4 + c_2 e_4) \tag{24}$$

If we use the following control input the sliding surface will be an attractive surface and Eq. (24) will be stable, which is analyzed in the Stability Analysis section.

$$\tau_v = -\frac{1}{X_u}\left(\Lambda_u \dot{\theta}^2 + \varphi_u g - u_d + c_1 e_2 + \alpha\left(\Lambda_u \dot{\theta}^2 + \psi_\gamma \dot{\gamma}^2 + X_\gamma \tau_v + \varphi_\gamma g - \dot{\gamma}_d + c_2 e_4\right)\right) - k_1 tanh(S) - k_2 S \tag{25}$$

The positive tuning parameters k_1 and k_2 are used to have a stable control algorithm. The chattering phenomena [26, 27], which are typical of systems controlled using SMC techniques, are high-frequency oscillations around the desired values that can be reduced using the saturation function instead of the discontinuous sign function. While there exist various approaches to address this issue, the Super-Twisting Algorithm (STA) stands out as a particularly compelling choice. Another solution to reduce chattering in SMC is to replace the sign function with a continuous and smooth function like the hyperbolic tangent (tanh) function. Using tanh instead of the sign function can make the control input smoother and more continuous. The readers who are interested in the mathematical descriptions of SMC for steering subsystem can refer to Appendix 2.

4.2.1 SMC Tuning and Results

In this subsection, the tuning of the parameters of the SMC algorithm will be discussed. Parameter tuning has been developed and tested both on the mathematical model implemented in Matlab and on the virtual prototype created in Adams. A sensitivity analysis has been carried out until reaching an optimum result with respect to the closed-loop system performance. The performance of the controller can be defined in relation to the reference trajectory assigned for the velocity.

Let it be recalled that three reference velocity profiles were defined in section 4.1 and labelled as:

– Case a
– Case b
– Case c

These references are used to represent different actions taken by the driver and are each characterized by increasing values of acceleration, deceleration, and peak velocity. As such it might be expected that the tracking performance will not be uniform. The parameters of the SMC controllers are obtained by trial and error. The tuned parameters are given as $c_1 = 0.01$, $c_2 = 1.5$, $k_1 = 2$ and $k_2 = 12$. In Fig. 10 obtained results for the sliding mode control with α technique in stabilization and velocity tracking in pure-Matlab and co-simulation with Adams are presented.

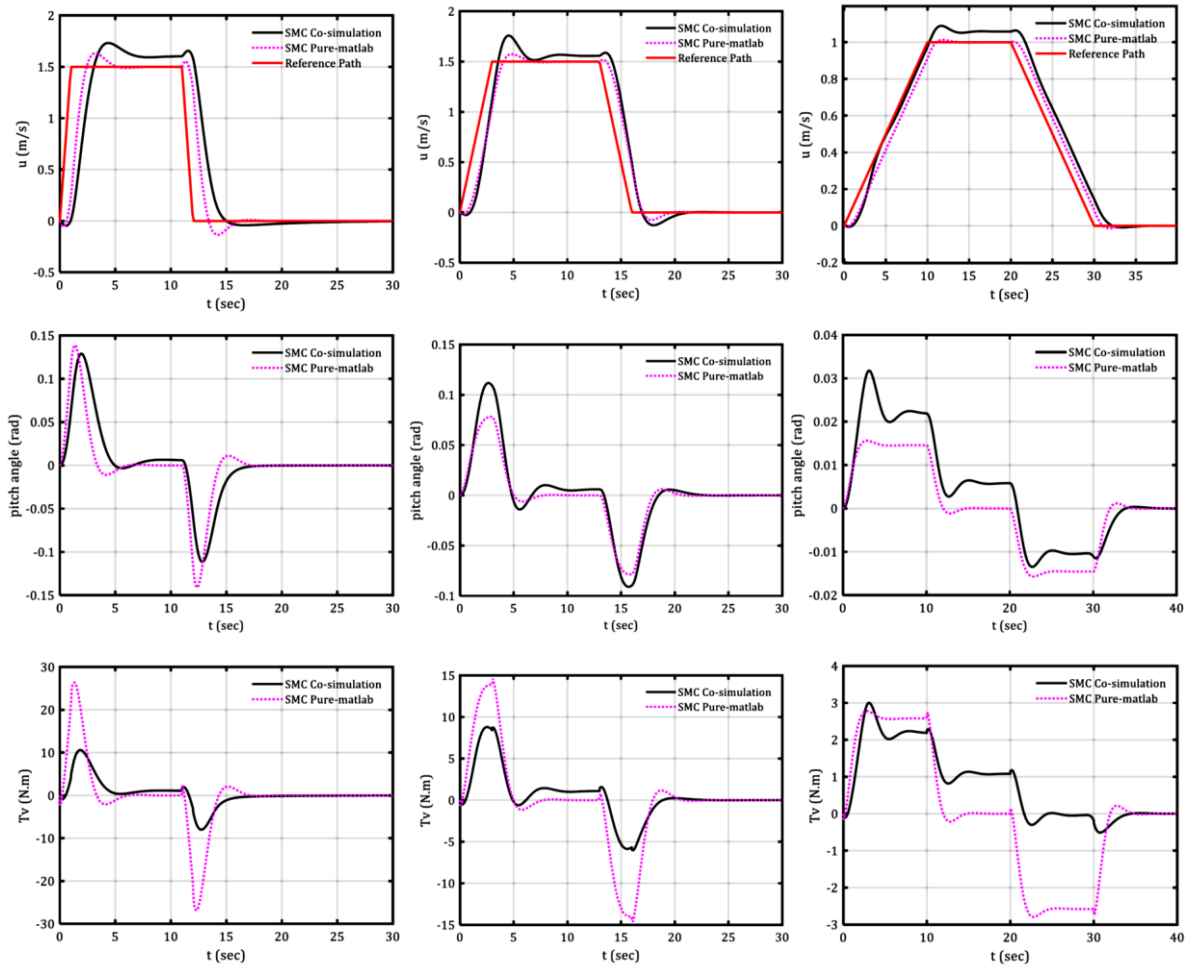

Fig. 10: Sliding mode control with α technique in stabilization and velocity tracking in pure-Matlab and co-simulation with Adams

As can be seen, the sliding mode control in both pure-Matlab and Adams-Matlab co-simulation using the α technique was able to track the reference velocity in different reference velocity profiles and stabilize the inclination angle well. The results in the pure-Matlab have the ideal state and show fewer errors, but because the real model with different effects and phenomena is present in Adams software, it represents more errors. In case a, which takes less time and is considered a more difficult profile, the amount of errors is higher, and in case c, which has better conditions in this respect, fewer tracking errors are seen. It can also be seen that in the stages where the velocity control is being carried out, the pendulum angle error has a limited value and when the reference velocity is followed, the inclination angle control has its ideal state and the angle reaches zero. The results for three different profiles show the proper performance of the sliding mode control along with the α technique.

4.3 Stability Analysis

The Lyapunov stability theorem utilizes a positive definite function called the Lyapunov function $V(x)$ to show that the system is stable if the time derivative of V (x) is negative definite [15]. Consider, for example, a continuous scalar function $V(x)$ that is 0 at the origin and positive elsewhere i.e. $V(0) = 0$ and $V(x) > 0$ for $x = 0$. Imagine the function $V(x)$ as an energy function; if the time derivative of $V(x)$ is negative, it can be implied that the energy is strictly decreasing over time, and all states will converge to zero. By utilizing the Lyapunov stability theory [21], we can prove the stability of the controlled closed-loop system composed by the plant and the SMC controller designed using the α technique. Eqs. (22) describes two surfaces suitable for these controlling purposes combined with the use of the coefficient α. Let the Lyapunov candidate function is considered as:

$$V_1 = \frac{1}{2}S^2 \tag{26}$$

It is clear that V_1 is positive definite (lpd). The first time derivative of V_1 can be calculated as

$$\dot{V}_1 = S\dot{S} = S(s_1 + \alpha s_2) \tag{27}$$

Substituting from (20, 21) into (34) results in

$$\dot{V}_1 = S\dot{S} = S(\dot{e}_2 + c_1 e_2 + \alpha(\dot{e}_4 + c_2 e_4)) \tag{28}$$

Substituting from (17, 19) into (35) yields

$$\dot{V}_1 = S(\Lambda_u \dot{\theta}^2 + \psi_u \dot{\gamma}^2 + X_u \tau_v + \varphi_u g - u_d + c_1 e_2 + \alpha(\Lambda_u \dot{\theta}^2 + \psi_\gamma \dot{\gamma}^2 + X_\gamma \tau_v + \varphi_\gamma g - \dot{\gamma}_d + c_2 e_4)) \tag{29}$$

After taking the time derivative $\dot{V}_1$ and substituting from Eq. (25), the control input τ_v cancels some terms so that $\dot{V}_1$ can be expressed as

$$\dot{V}_1 = S(-k_1 tanh(S) - k_2 S) = -k_1|S| - k_2 S^2 \tag{30}$$

Finally, $\dot{V}_1$ becomes negative definite. It is confirmed that by providing the condition $S\dot{S} < 0$ the sliding surface $S = 0$ is an attractive surface that guarantees the stability of the sliding mode controller [16]. We have considered only SMC surfaces of the tilt angle and the longitudinal velocity of TWSBV for the SIMO subsystem. In order to prove the Lyapunov-based stability of the whole system, the steering subsystem which is single-input, single-output (SISO) should also be considered. Consider the Lyapunov function candidate for the yaw angle controller as

$$V_2 = \frac{1}{2} s_3^2 \tag{31}$$

The derivative of the Lyapunov function candidate and using Eq. (31) results in

$$\dot{V}_2 = s_3 \dot{s}_3 = s_3(\Lambda_\theta \dot{\theta} u + \psi_\theta \dot{\gamma} \dot{\theta} + X_\theta \tau_\omega - \ddot{\theta}_d + c_3 \dot{e}_5) \tag{32}$$

After taking the time derivative of V_2 and substituting from Eq. (32), the control input τ_w can be used to cancel some of the terms in $\dot{V}_2$, and it can be expressed as

$$\dot{V}_2 = s_3(k_5 tanh(s_3) - k_6 s_3) = -k_3|s_3| - k_4 s_3^2 \tag{33}$$

Finally, $\dot{V}_2$ becomes negative definite. It is confirmed that by providing the condition $s_3 \dot{s}_3 < 0$ the sliding surface $s_3 = 0$ is an attractive surface that guarantees the properties of stability and robustness of the SMC controller. Consider that the TWSBV dynamic model of the system has two separated decoupled algebraically independent subsystems: one is the longitudinal motion subsystem while the other is the steering subsystem. For each subsystem we applied the Lyapunov theorem; the general Lyapunov function of the overall system is the summation of both Lyapunov functions of two subsystems [22].

$$V = V_1 + V_2 = \frac{1}{2} S^2 + \frac{1}{2} s_3^2 \tag{34}$$

By calculating the derivative of the Lyapunov function as follows

$$\dot{V} = \dot{V}_1 + \dot{V}_2 = -k_1|S| - k_2 S^2 - k_3|s_3| - k_4 s_3^2 \tag{35}$$

Since both $\dot{V}_1$ and $\dot{V}_2$ are negative definite, so is $\dot{V}$. The stability of the overall system is thus proven.

4.4 Feedback Linearization Method

In this section, the developed nonlinear dynamic model has been used in order to design a model-based Feedback Linearization (FL) controller for the under-actuated TWSBV. We will start by discussing the concepts of feedback linearization and then we will show how to utilize this method for controlling the TWSBV. The feedback linearization method uses nonlinear state feedback in order to obtain closed-loop stable linear dynamics [5]. These linear dynamics can then be easily regulated using an outer control loop designed using classical techniques. First, the dynamic equation of the system is written as

$$x^{(n)} = f(x) + b(x)u \tag{36}$$

where u is the scalar input, $x = [x, \dot{x}, \ldots, x^{(n-1)}]$ is the state vector, and $f(x)$ and $b(x)$ are nonlinear functions of system states. Assuming that b is non-zero, we can obtain the open-loop relationship between input and states as below:

$$u = \frac{1}{b}(v - f) \tag{37}$$

According to the feedback linearization method, the internal control loop input v is defined as follows:

$$x^{(n)} = v \tag{38}$$

Thus, the internal control loop input v can be chosen as

$$v = -k_0 x - k_1 \dot{x} - k_{n-1} x^{(n-1)} \tag{39}$$

Therefore, according to Eq. (49) v is defined as a state feedback controller [23]. Let us utilize this interesting above-mentioned approach for designing the FL controller for the TWSBV. Firstly by choosing a state representation of the system, the transformation of a non-linear dynamic system into a linear one can be realized. Considering the nonlinear dynamic equations of the system with the α technique can be rewritten as

$$\dot{u} + \alpha \ddot{\gamma} = A + B \tau_v \tag{40}$$

where A and B are nonlinear functions of states and nonzero. The dynamic equations are simplified through feedback linearization. In order to cancel the nonlinear terms and impose the desired closed-loop linear dynamics, the system can be represented as

$$\tau_v = \frac{1}{B}(\dot{u} + \alpha\ddot{\gamma} - A) \tag{41}$$

By Eq. (41) the nonlinearities can be cancelled, and we can obtain a simple linear relationship between the outputs and the input. Designing the outer control loop for tracking velocity reference and balancing the whole system controller can be done by choosing $\dot{u}$ and $\ddot{\gamma}$ as follows:

$$\dot{u} = \dot{u}_d - k_0(u - u_d) \tag{42}$$

$$\ddot{\gamma} = \ddot{\gamma}_d - k_1(\gamma - \gamma_d) - k_2(\dot{\gamma} - \dot{\gamma}_d) \tag{43}$$

By using the α technique:

$$\dot{u} + \alpha \ddot{\gamma} = \dot{u}_d - k_0 e_2 + \alpha (\ddot{\gamma}_d - k_1 e_3 - k_2 e_4) \tag{44}$$

Thus, the following control law is obtained:

$$\tau_v = \frac{1}{B}(\dot{u}_d - k_0 e_2 + \alpha (\ddot{\gamma}_d - k_1 e_3 - k_2 e_4) - A) \tag{45}$$

This controller can be easily implemented, and numerical results show that the designed method works effectively. The control block diagram is depicted in Fig. 11. Obtained results both in pure-Matlab and the Adams-Matlab co-simulation of the feedback linearization method for the TWSBV system are presented in Fig. 12 both for pure-Matlab and for the Adams-Matlab co-simulation. It can be seen that both tracking velocity reference and balancing are achieved.

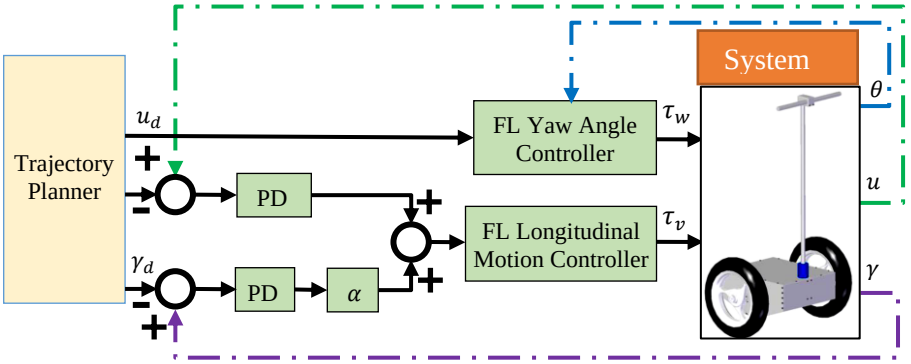

Fig. 11: Schematic block diagram of feedback linearization with α technique controller

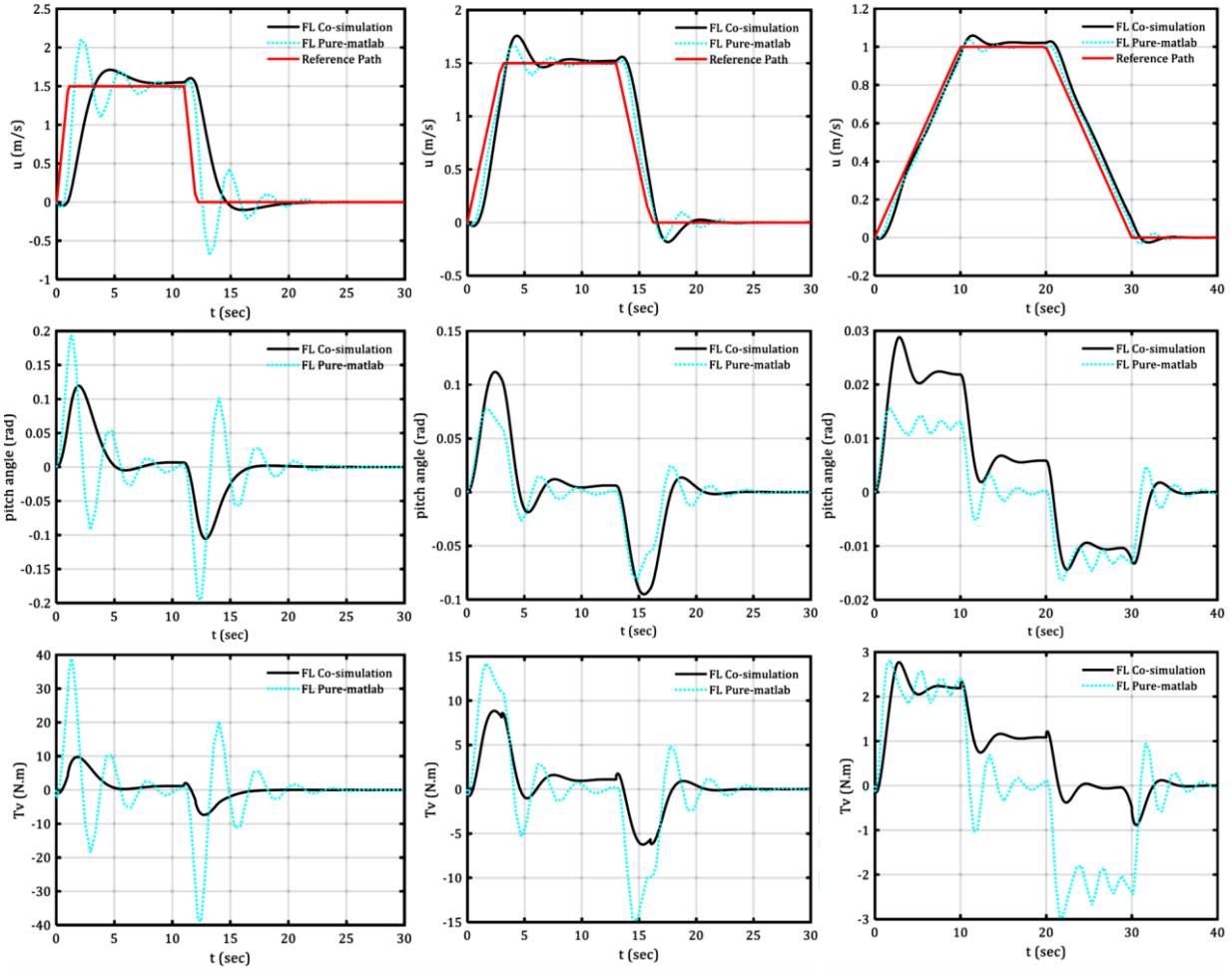

Fig. 12: Feedback linearization control with α technique in stabilization and velocity tracking in pure-Matlab and co-simulation with Adams

As can be seen, the feedback linearization control in both pure-Matlab and Adams-Matlab co-simulation using the α technique was able to track the reference velocity in different reference velocity profiles and stabilize the inclination angle well. In case a, which takes less time and is considered a more difficult profile, the amount of errors is higher, and in case c, which has better conditions in this respect, fewer tracking errors are seen. It can also be seen that in the stages where the velocity control is being carried out, the inclination angle error has a limited value and when the reference velocity is followed, the pendulum angle control has its ideal state and the angle reaches zero. The results for three different profiles show the proper performance of the feedback linearization along with the α technique.

4.5 PID Control

In this section, the Proportional-integral-derivative (PID) controller [24] has been investigated owing to its simplicity and effectiveness in many technical and industrial applications. The PID controller has three control parameters, k_p, k_i and k_d which are called the proportional, the integral, and the derivative gains, respectively. To stabilize the TWSBV and to track the longitudinal reference velocity, two parallel PID controllers have been employed. The outputs of the two controllers are combined by using the α technique, in such a way that the tilt control task is overall prioritized. The general parallel structure of controllers and the α technique are shown in Fig. 13. At the mathematical level the resulting control signal is therefore described as

$$\tau_u = k_p e_2(t) + k_i \int e_2(t) + k_d \dot{e}_2(t) \tag{46}$$

$$\tau_\gamma = k_p e_3(t) + k_i \int e_3(t) + k_d \dot{e}_3(t) \tag{47}$$

$$\tau_v = \tau_u + \alpha \tau_\gamma \tag{48}$$

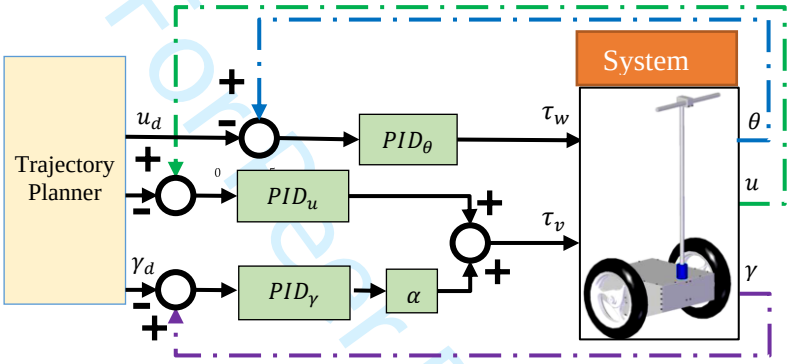

Fig. 13: Closed loop control system block diagram

The validation of the tracking performance is done in three different scenarios. As attested by the pure-Matlab simulation and Adams-Matlab co-simulation results reported in Fig. (14), the PID controller can effectively satisfy the two combined purposes, i.e. tracking the velocity reference and balancing the TWSBV at the same time. Fig. 14 demonstrates that during the acceleration and deceleration phases, the controller takes care of decreasing the velocity error. Soon after reaching the constant cruise velocity value, the PID controller is also able to guarantee convergence of the tilt angle error to zero. As can be seen, the PID control could smoothly follow the Case c reference profile. It means that it has had enough time to stabilize the system and track the reference velocity.

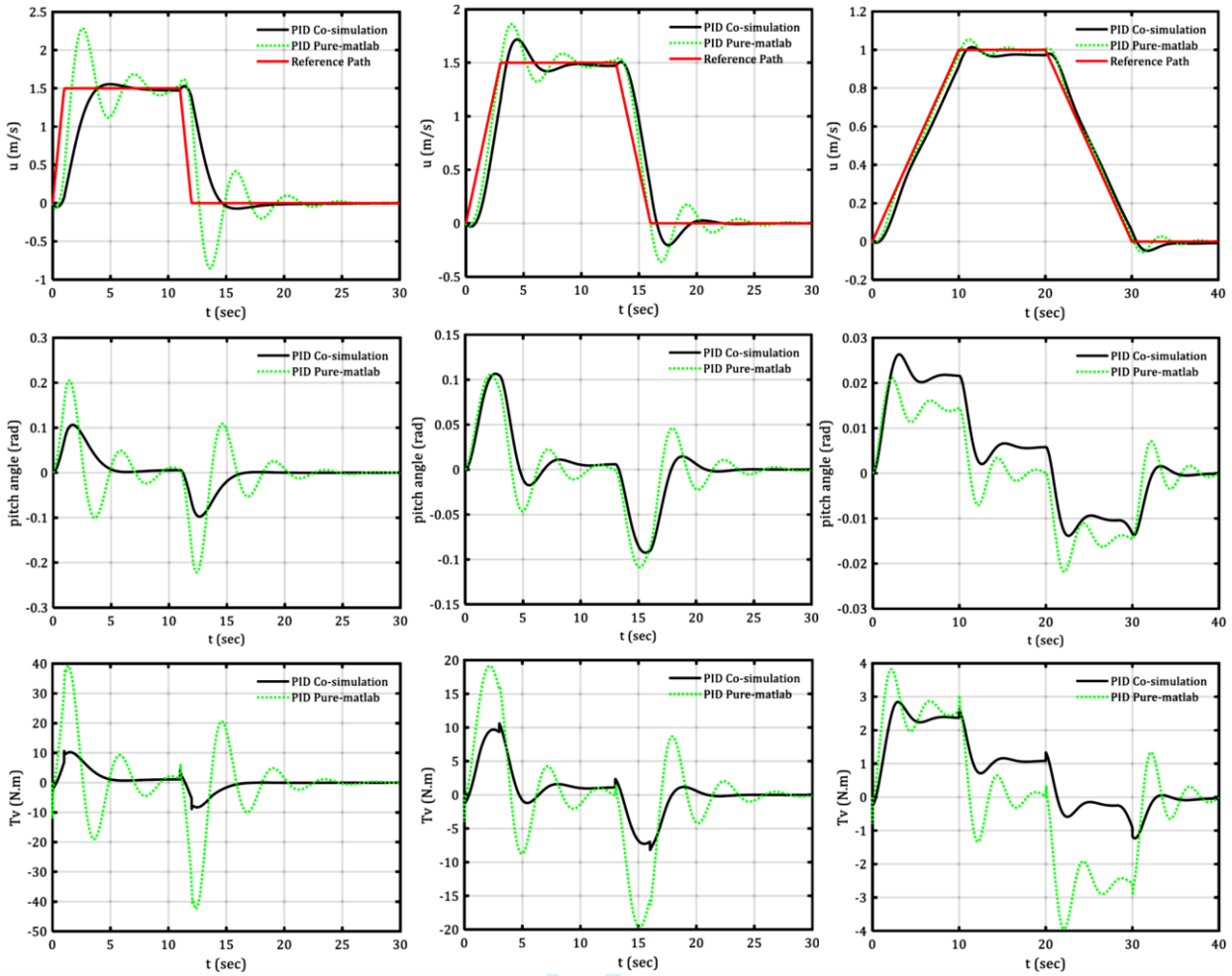

Fig. 14: PID control with α technique in stabilization and velocity tracking in pure-Matlab and co-simulation with Adams

As can be seen, the PID control in both pure-Matlab and Adams-Matlab co-simulation using the α technique was able to track the reference velocity in different reference velocity profiles and stabilize the inclination angle well. In case a, which takes less time and is considered a more difficult profile, the amount of errors is higher, and in case c, which has better conditions in this respect, fewer tracking errors are seen. It can also be seen that in the stages where the velocity control is being carried out, the pendulum angle error has a limited value and when the reference velocity is followed, the inclination angle control has its ideal state and the angle reaches zero. The results for three different profiles show the proper performance of the PID control along with the α technique.

4.6 LQR Control

This subsection presents the development of an LQR controller based on the α technique. In order to show the advantages or disadvantages of the designed LQR controllers for the TWSBV we need to evaluate the closed-loop performance of the system with the designed longitudinal reference profiles. The full-state feedback controller with the LQR method [25] gives promising results. The equations of the linearized longitudinal sub-system are rearranged into a state space formulation in order to deploy LQR methods.

In order to define the relative weight between longitudinal speed and pitch errors, a new definition as below by the α technique can be employed. Linear control techniques developed for fully-actuated systems cannot be used directly to stabilize the underactuated TWSBV system. The linear model for the TWSBV can be easily obtained in the form $\dot{x} = Ax + Bu$. It is clear that the inclination angle γ is controlled by the torque τ_v and the longitudinal velocity u cannot be controlled in isolation, meaning that the inclination angle of the vehicle has a direct influence on the longitudinal velocity. The α technique is applied to the minimal representation of the system in order to introduce a new state variable defined as a linear combination of longitudinal velocity and rate of change of pitch angle. The linear quadratic regulator derives closed-loop

pole locations which are the optimal pole locations with respect to an energy cost function that can guarantee the desired closed-loop performance of the system. The LQR controller consists of a feedback gain matrix K, which will be generally used to implement the control input $u = -Ke$ as

$$u = -K\begin{bmatrix} e_3 \\ e_4 \\ e_2 + \alpha e_4 \end{bmatrix} \tag{49}$$

where K is the gain matrix defined as

$$u = -R^{-1}B^T Px \tag{50}$$

Here P is a positive definite matrix which is solved from the following Algebraic Riccati Equation (ARE).

$$A^T P + PA - PBR^{-1}B^T P + Q = 0 \tag{51}$$

For achieving the optimal response, weight matrices Q and R are selected by the designer. The Q matrix contains weighted values for states. These values should be allocated according to the relative importance of each state. It is important to remember that a higher value in the Q matrix implies a higher level of regulation and prioritization of the affected state variables. The R matrix elements act like input weights, which can affect the amount of controller input signal. The LQR method minimizes a performance index defined as:

$$J = \frac{1}{2}\int_0^\infty \{x^T Qx + u^T Ru\}dt \tag{52}$$

The design key to find the right weight matrix Q and matrix R are based on the empirical tuning:

$Q = diag[1\ 2\ 10], R = 1$

In Fig. 15 obtained results for the LQR method with α technique in stabilization and velocity tracking in pure-Matlab and co-simulation with Adams are presented.

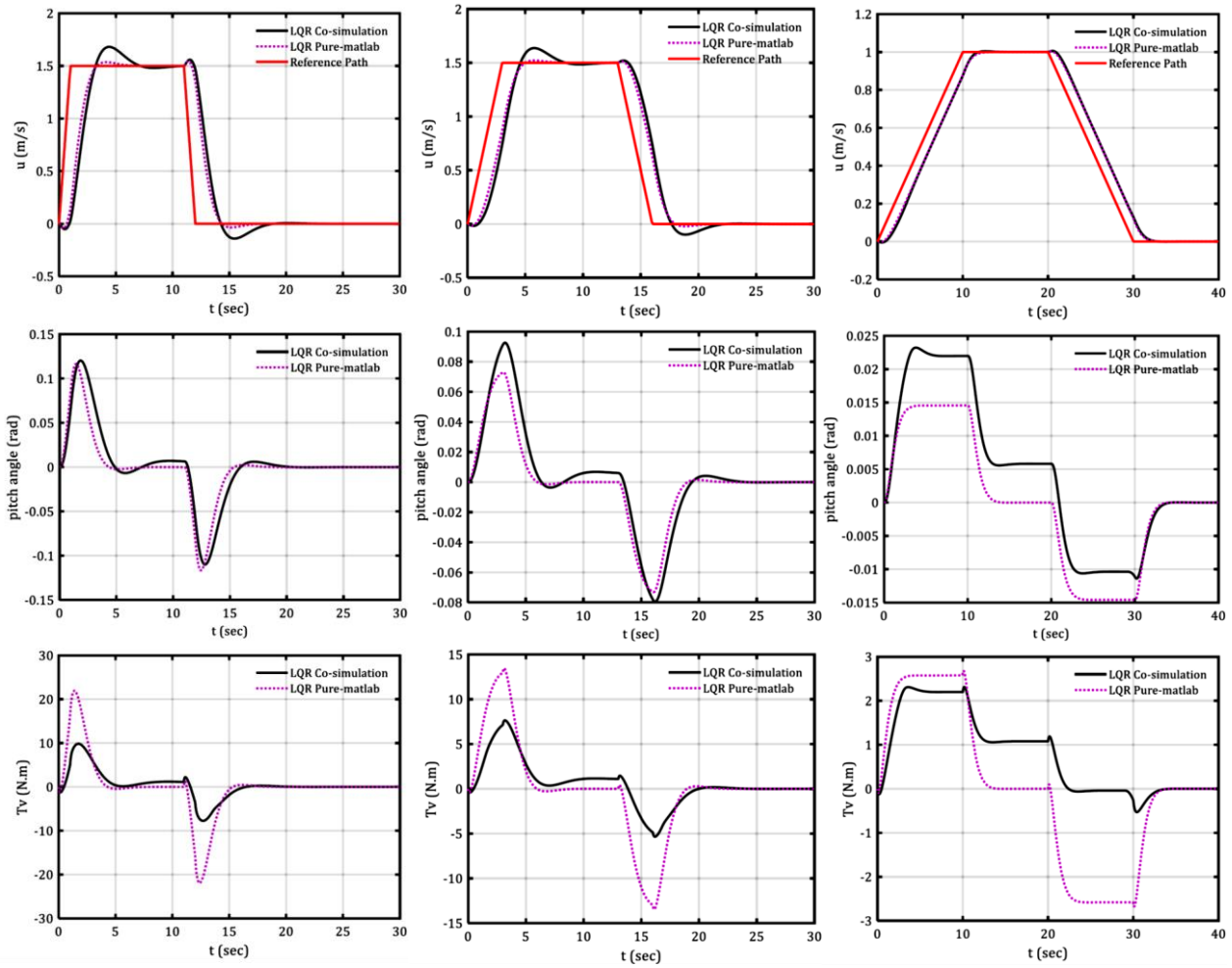

Fig. 15: LQR control with α technique in stabilization and velocity tracking in pure-Matlab and co-simulation with Adams

As can be seen, the LQR control in both pure-Matlab and Adams-Matlab co-simulation using the α technique was able to track the reference velocity in different reference velocity profiles and stabilize the inclination angle well. In case a, which takes less time and is considered a more difficult profile, the amount of errors is higher, and in case c, which has better conditions in this respect, fewer tracking errors are seen. It can also be seen that in the stages where the velocity control is being carried out, the pendulum angle error has a limited value and when the reference velocity is followed, the inclination angle control has its ideal state and the angle reaches zero. The results for three different profiles show the proper performance of the LQR control along with the α technique.

4.7 Tuning the α parameter

Obtained results for tuning the α parameter for the sliding mode control in stabilization and velocity tracking in pure-Matlab and co-simulation with Adams are presented in Fig. 16.

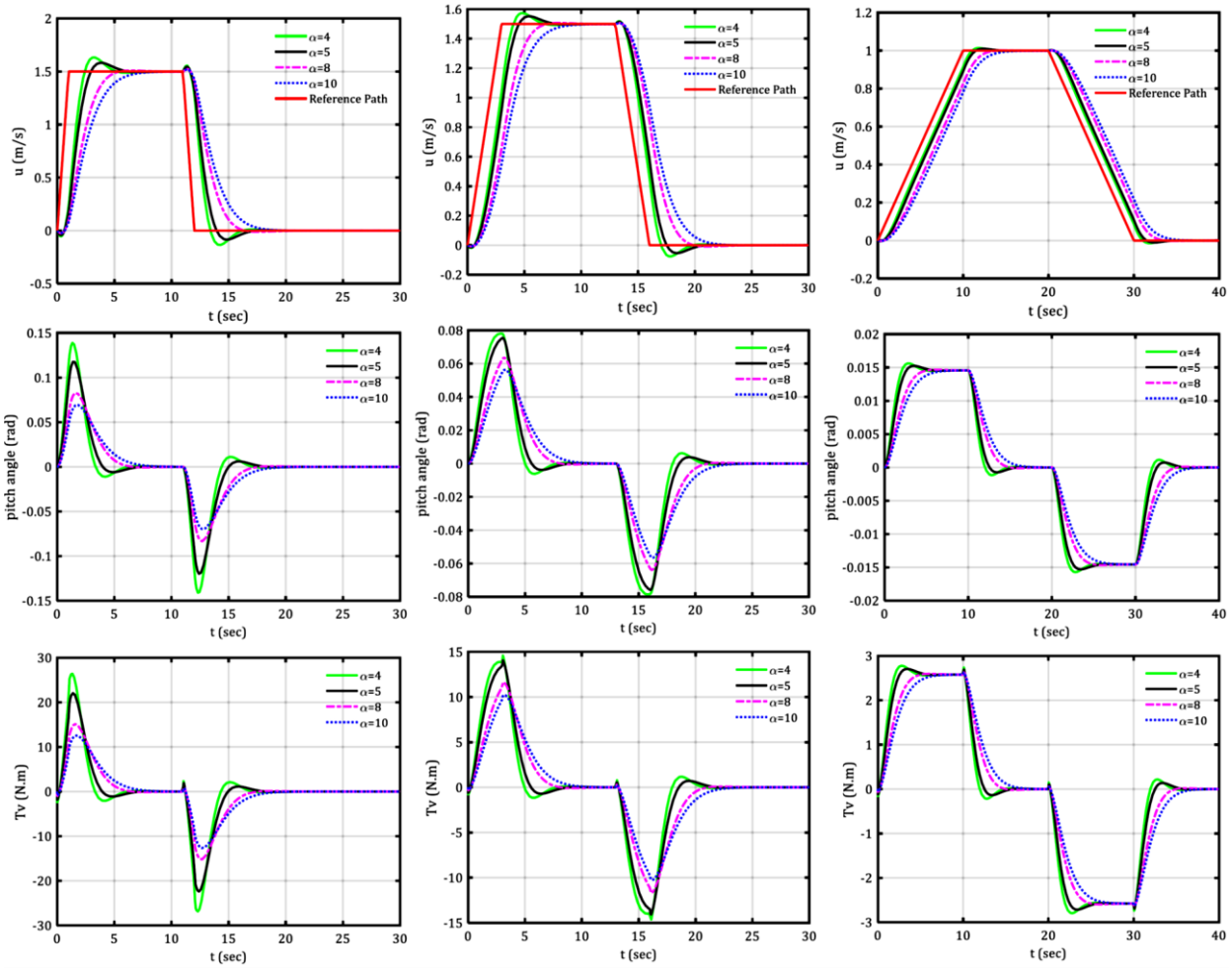

Fig. 16. Comparison of performance for tracking the motion profiles with different α values using sliding mode controller

The SMC controller tries to prevent the degradation of the closed loop performance, which occurs during sudden acceleration in one second and deceleration in one second. It is remarkable that increasing α directly can amplify the weight and priority of the balancing task but on the other hand can weaken the ability to follow the reference longitudinal velocity. For example in Case a, it is easily understandable that by increasing the value of α balancing has been improved but on the other side the velocity tracking has been confronted with a significant reduction in performance. The different motion profiles for reference trajectories are generated that comply with human driver requirements by exposing him/her to acceptable levels of accelerations, decelerations, and peak velocities. It is obvious that in case b the performance becomes better in comparison with case a. As can be seen, for α = 4 shortest settling time for the longitudinal velocity is visible. In the third scenario, on the other hand, the vehicle can smoothly follow the reference trajectory, given

the better matching between the required accelerations and the vehicle's capabilities. As the sliding surface using α technique and the linear relationship between the tilt angle and longitudinal velocity surfaces, the TWSBV can eventually reach the target of reference velocity. Even though the vehicle reaches the target velocity smoothly, it takes 12s to achieve the stable state and during the whole process, the stability of the vehicle has been guaranteed by the pitch variable being close to zero.

5. Summary and Conclusion

This paper provides the modelling and control of the non-linear underactuated two-wheeled self-balanced vehicle. The equations of motion are obtained based on the Lagrange method and non-holonomic constraints. The α technique is presented in order to simultaneously stabilize the velocity tracking error and the inclination angle of the TWSBV. Moreover, several controllers were developed based on the proposed α technique in the pure-Matlab environment. The aim was to stabilize the TWSBV around the unstable equilibrium configuration while also providing trajectory-tracking abilities. In parallel, the MSC Adams software has been utilized in order to model the vehicle as a multi-body system in which the tire-ground interactions are modelled in greater detail.

According to the similarities between the obtained results in both pure-Matlab model and co-simulation Adams-Matlab model, we can conclude that the mathematical model describes reasonably well the behavior of the real TWSBV. We remark that the controllers are based on the mathematical model featuring the assumption of pure rolling without slipping, by which the plant model assumes a manageable analytical form. On the contrary in the Adams model the slipping condition and road-tire model and reaction forces have been modeled. The Adams model has been developed to provide a virtual dynamic prototype of the TWSBV to detect any undesirable effect of the controller before the testing phase on the actual TWSBV prototype.
A brief outline of this document is as follows: section 2 provides detailed dynamic model of TWSBV which used throughout this research. In section 3 the Adams model introduced and also technical specification of various part of TWSBV have been presented. In section 4 deals with the control methodology to achieve desired performance, results of each designed controller based on pure-Matlab and Adams-Matlab co-simulation are discussed in the relevant subsections. The study is concluded in summary in order to providing general overview for reader. SMC method is especially attractive since its capability to handle nonlinear systems and disturbances, while SMC offers several advantages, such as robustness and good tracking performance; but in other hand chattering phenomena is a well-known disadvantage of sliding mode control. Feedback linearization relies on accurate models of the system dynamics. Therefore, developing an accurate model of a complex system can be challenging. However, in our case the friction effects are neglected to simplify the feedback linearization controller which causing an undesirable performance. The main distinguishing feature on the performance of SMC can be observed, is in the most severe conditions (Fig. 10). It means SMC controller is to prevent the degradation of the closed loop performances, which occur during sudden acceleration in one second and deceleration in one second. Moreover, as shown in Fig. 12, FL controller performance results have shown that in Case A leads to oscillation and poor stabilization of the vehicle. As it might be expected, given the discrepancies between the two models, the co-simulations tend to highlight a deterioration of the performance of the controller if compared with the results provided by the pure-Matlab analysis. Adams-Matlab co-simulation represents a highly useful intermediate step between the design of the controller and its experimental validation on a physical prototype. it is observed that LQR offers steady-state error during tracking longitudinal velocity and also requires a linear model to get an adequately controlled system. Also the accurate determination and tuning of the PID parameters could be challenging, finding appropriate parameters. By comparing Tab.5, which reports the results for the Case A,Tab.6 which is relative to Case B and Tab.7 which is relative to Case C; it is clear that MAE and RMSE in both variables inclination angle and longitudinal velocity are provided.

Table 5: The Motion Profile Parameters

Motion cases A	$RMS(e_u)$	$Max\|e_u\|$	$RMS(e_\gamma)$	$Max\|e_\gamma\|$
SMC	0.393	1.25	0.042	0.121
FL	0.394	1.30	0.048	0.140
PID	0.368	1.23	0.055	0.167
LQR	0.394	1.35	0.046	0.153

Table 6: The Motion Profile Parameters

Motion cases B	$RMS(e_u)$	$Max\|e_u\|$	$RMS(e_\gamma)$	$Max\|e_\gamma\|$
SMC	0.206	0.506	0.279	0.650
FL	0.217	0.533	0.327	0.072
PID	0.193	0.458	0.039	0.096
LQR	0.259	0.632	0.030	0.073

Table 7: The Motion Profile Parameters

Motion cases C	$RMS(e_u)$	$Max\|e_u\|$	$RMS(e_\gamma)$	$Max\|e_\gamma\|$
SMC	0.060	0.100	0.0099	0.0157
FL	0.069	0.110	0.0084	0.0133
PID	0.039	0.090	0.0104	0.0194
LQR	0.083	0.126	0.0098	0.0149

In this research authors tried to briefly introduces and analyses some commonly used controllers such as PID, LQR, FL, SMC for a TWSBV. This study's main contribution is a comprehensive discussion that includes the advantages and the limitations of the mentioned controllers to provide a proper understanding that may help the user to choose a suitable one.

6. Further Research

The future perspectives of this dissertation include the modeling of the terrain surface as accurately as possible. There is a gap between even surface models and actual vehicle performance on uneven surfaces, as the driver, while using the TWSBV for outdoor activity, is always affected by several phenomena such as unknown terrain, inclination angle, changing slope and external disturbances. In order to deal with the above mentioned phenomena, we foresee improvements within the Adams surface models. By focusing on modeling different terrain profiles, vehicle maneuverability over several terrain types can be analyzed. Moreover to enhance the ground surface model, sloped terrain can be incorporated within the TWSBV simulation. Additionally road disturbances can be further investigated and finally a disturbance observer can be designed in order to specifically increase the vehicle performance.

7. Appendix 1

In equations of motion of the TWSBV Eqs. (4-6) mentioned parameters are defined as:

$$\Lambda_u = \frac{-B_u C_\gamma - A_\gamma C_u}{A_u A_\gamma - B_u B_\gamma} \tag{53}$$

$$\psi_u = -\frac{C_u A_\gamma}{A_u A_\gamma - B_u B_\gamma} \tag{54}$$

$$X_u = \frac{\frac{A_\gamma}{r_\omega} + B_u}{A_u A_\gamma - B_u B_\gamma} \tag{55}$$

$$\varphi_u = \frac{B_u D_\gamma}{A_u A_\gamma - B_u B_\gamma} \tag{56}$$

$$\Lambda_\gamma = \frac{-C_\gamma A_u + B_u C_u}{A_u A_\gamma - B_u B_\gamma} \quad (57)$$

$$\psi_\gamma = \frac{B_\gamma C_u}{A_u A_\gamma - B_u B_\gamma} \quad (58)$$

$$X_\gamma = \frac{\frac{B_\gamma}{r_\omega} + A_u}{A_u A_\gamma - B_u B_\gamma} \quad (59)$$

$$\varphi_\gamma = -\frac{A_u D_\gamma}{A_u A_\gamma - B_u B_\gamma} \quad (60)$$

$$\Lambda_\theta = \frac{B_\theta}{A_\theta} \quad (61)$$

$$\psi_\theta = \frac{C_\theta}{A_\theta} \quad (62)$$

$$X_\theta = \frac{D_\theta}{A_\theta} \quad (63)$$

$$A_u = 3m_\omega + m_{ch} \quad (64)$$

$$B_u = hm_{ch}cos\gamma \quad (65)$$

$$C_u = -hm_{ch}sin\gamma \quad (66)$$

$$A_\gamma = I_{yy_{ch}} + m_{ch}h^2 \quad (67)$$

$$B_\gamma = hm_{ch}cos\gamma \quad (68)$$

$$C_\gamma = -\frac{1}{2}\left[I_{xx_{ch}} + m_{ch}h^2 - I_{zz_{ch}}\right]sin2\gamma \quad (69)$$

$$D_\gamma = -hm_{ch}sin\gamma \quad (70)$$

$$A_\theta = \left[2(m_\omega l^2 + I_{2\omega}) + I_{xx_{ch}}sin^2\gamma + m_{ch}h^2sin^2\gamma + I_{zz_{ch}}cos^2\gamma + m_\omega l^2\right] \quad (71)$$

$$B_\theta = -m_{ch}hsin\gamma \quad (72)$$

$$C_\theta = -\left(m_{ch}h^2 + I_{xx_{ch}} - I_{zz_{ch}}\right)sin2\gamma \quad (73)$$

$$D_\theta = \frac{1}{r_\omega} \quad (74)$$

8. Appendix 2

The focus of our discussion remains centered on the core aspects of designing controller for longitudinal motion of TWSBV. However, for the benefit of interested readers, the detailed formula for steering subsystem controller has been thoughtfully provided in the appendix 2. The steering subsystem which is a single-input, single-output (SISO) should also be considered as

$$\ddot{\theta} = \Lambda_\theta \dot{\theta}^2 \boldsymbol{u} + \Psi_\theta \dot{\theta}\dot{\gamma} + X_\theta \tau_w \quad (75)$$

The yaw state error and yaw rate error are defined as $e_5 = \theta - \theta_d$, $e_6 = \dot{\theta} - \dot{\theta}_d$ where θ_d is the desired

yaw angle. The error differential equation can be expressed as:

$$\dot{e}_5 = e_6 \quad (76)$$

$$\dot{e}_6 = \Lambda_\theta \dot{\theta}^2 u + \Psi_\theta \dot{\theta}\dot{\gamma} + X_\theta \tau_w - \ddot{\theta}_d \quad (77)$$

If we use the conventional sliding surfaces as below:

$$s_3 = \dot{e}_5 + c_3 e_5, \quad c_3 > 0 \quad (78)$$

In order to maintain s_3 at a constant value, therefore $ds_3(t)/dt = 0$.

$$\dot{s}_3 = \dot{e}_6 + c_3 \dot{e}_5 \quad (79)$$

Substituting from Eq. (78) into Eq. (80) yields:

$$\dot{s}_3 = \Lambda_\theta \dot{\theta}^2 u + \Psi_\theta \dot{\theta}\dot{\gamma} + X_\theta \tau_w - \ddot{\theta}_d + c_3 \dot{e}_5 \quad (80)$$

If we use the following control input the sliding surface will be

$$\tau_\omega = \frac{1}{X_\theta}(-\Lambda_\theta \dot{\theta} u - \psi_\theta \dot{\gamma}\dot{\theta} + \ddot{\theta}_d - c_3 \dot{e}_5 - k_3 tanh(s_3) - k_4 s_3) \quad (81)$$

The positive control gains k_3 and k_4 are used to have a stable control algorithm.

Steering Subsystem control discussion

In previous sections, the yaw angle is stabilized around zero. In this section in addition to longitudinal control based on the α technique, the yaw angle control is successfully tracked a reference trajectory. Obtained results in tracking a reference sinusoidal trajectory are shown in Fig. 17.

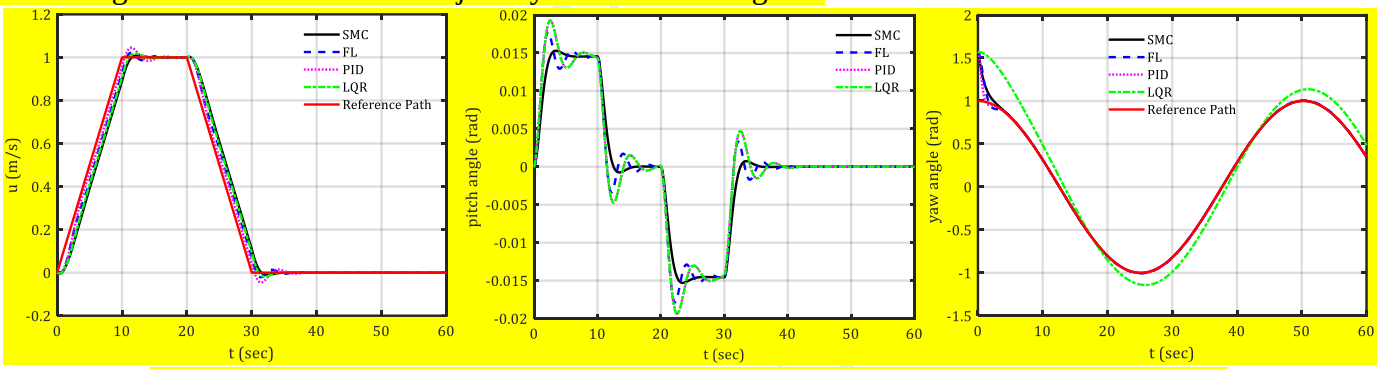

Fig. 17: Yaw angle control in tracking a reference trajectory along with longitudinal control

The results demonstrate that the system's yaw angle can effectively track a sinusoidal reference trajectory while maintaining longitudinal control. This indicates that the proposed control approach is effective in simultaneously controlling both the yaw angle and longitudinal behavior of the system.

Author Contributions

Authors (A.G., P.R., and R.S.) contributed equally. All authors have discussed and analyzed the results and reviewed the manuscript.

Competing interests

The authors declare no competing interests.

Data Availability

No datasets were generated or analyzed during the current study.

9. List of Symbols

Mathematical Symbols

c_z	Vertical damping
d	Tire deformation
f_v	Rolling resistance coefficient

F_x	Longitudinal force
F_y	Lateral force
g	Gravity Acceleration
h	Distance from the half distance between to wheels to the centre of gravity of the chassis
$I_{yy_{ch}}$	Inertia moment of the chassis about the $Y_{3_{ch}}$
$I_{xx_{ch}}$	Inertia moment of the chassis about the $X_{3_{ch}}$
$I_{zz_{ch}}$	Inertia moment of the chassis about the $Z_{3_{ch}}$
I_{w1}	Inertia moment of the chassis about the $X_{3_{ch}}$
I_{w2}	Inertia moment of the chassis about the $Y_{3_{ch}}$
k_p, k_i, k_d	Proportional, integral, and derivative gains
k_α	Cornering stiffness coefficient
k_y	Lateral stiffness
k_z	Vertical stiffness
l	Half of the distance between the wheels
m_{ch}	Mass of chassis (mass of driver is included)
m_w	Mass of the wheel
P	Positive-definite matrix
Q, R	Weight matrices
r_w	The radius of the wheel
$s(t)$	Sliding surface
u_0, u_f	The initial and final velocity
u_m	Maximal velocity
v_{sx}	Slip speed
v_z	Deformation speed
v_{μ_s}	The velocity of the static friction coefficient
v_{μ_d}	The velocity of the dynamic friction coefficient
V	Lyapunov function candidate
x, y	The position coordinates of the system in X–Y plane

Greek Symbols

α	Control gain
Ω	Angular speed
μ_s	Static friction coefficient
μ_d	Dynamic friction coefficient
τ_1, τ_2	Torques of left and right wheels
τ_v	Torque input for longitudinal motion
τ_w	Torque input for yaw motion
φ_1, φ_2	Rotational angles of the left and right wheels
θ	Yaw angle of TWSBV
γ	The inclination angle of TWSBV

10. References

[1] A. Ghaffari, A. Shariati, and A. H. Shamekhi, "A modified dynamical formulation for two-wheeled self-balancing robots," Nonlinear Dynamics, vol. 83, no. 1, pp. 217-230, 2016/01/01 2016, doi: 10.1007/s11071-015-2321-9.

[2] Y. Kim, S. H. Kim, and Y. K. Kwak, "Dynamic Analysis of a Nonholonomic Two-Wheeled Inverted Pendulum Robot," Journal of Intelligent and Robotic Systems, vol. 44, no. 1, pp. 25-46, 2005/09/01 2005, doi: 10.1007/s10846-005-9022-4.

[3] K. M. Goher and M. O. Tokhi, "A New Configuration of Two-Wheeled Inverted Pendulum: A Lagrangian-Based Mathematical Approach," 2010.

[4] N. Sophan Wahyudi, "Real-Time Control System for a Two-Wheeled Inverted Pendulum Mobile Robot," in Advanced Knowledge Application in Practice, F. Igor Ed. Rijeka: IntechOpen, 2010, p. Ch. 16.

[5] K. Pathak, J. Franch, and S. K. Agrawal, "Velocity and position control of a wheeled inverted pendulum by partial feedback linearization," IEEE Transactions on Robotics, vol. 21, no. 3, pp. 505-513, 2005, doi: 10.1109/TRO.2004.840905.

[6] V. B. V. Nghia, T. Van Thien, N. N. Son, and M. T. Long, "Adaptive neural sliding mode control for two wheel self balancing robot,"International Journal of Dynamics and Control, vol. 10, no. 3, pp. 771-784, 2022.

[7] W. Junfeng, L. Yuxin, and W. Zhe, "A robust control method of two-wheeled self-balancing robot," in Proceedings of 2011 6th International Forum on Strategic Technology, 22-24 Aug. 2011 2011, vol. 2, pp. 1031-1035, doi: 10.1109/IFOST.2011.6021196.

[8] I. Chawla, V. Chopra, and A. Singla, "Robust stabilization control of a spatial inverted pendulum using integral sliding mode controller," International Journal of Nonlinear Sciences and Numerical Simulation, vol. 22, no. 2, pp. 183-195, 2021, doi: doi:10.1515/ijnsns-2018-0029.

[9] L. Guo, S.A. Asad Rizvi and Z. Lin, "Optimal control of a two-wheeled self-balancing robot by reinforcement learning," International Journal of Robust and Nonlinear Control, 2021

[10] L. Chen et al., "Robust hierarchical sliding mode control of a two-wheeled self-balancing vehicle using perturbation estimation," Mechanical Systems and Signal Processing, vol. 139, p. 106584, 2020/05/01/ 2020, doi: https://doi.org/10.1016/j.ymssp.2019.106584.

[11] M. S. Arani, H. Ebrahimi Orimi, W.-F. Xie, and H. Hong, "Sliding Mode Control Design of a Two-Wheel Inverted Pendulum Robot: Simulation, Design and Experiments," in Advances in Motion Sensing and Control for Robotic Applications, Cham, F. Janabi-Sharifi and W. Melek, Eds., 2019// 2019: Springer International Publishing, pp. 93-107.

[12] S. Liang, Z. Wang, and G. Stepan, "Motion control of a two-wheeled inverted pendulum with uncertain rolling resistance and angle constraint based on slow-fast dynamics," Nonlinear Dynamics, vol. 104, no. 3, pp. 2185-2199, 2021/05/01 2021, doi: 10.1007/s11071-021-06439-7.

[13] V. T. Nguyen et al.,"Optimized PID Controller for Two-wheeled self-balancing Robot based on the Genetic Algorithm", Springer 2023

[14] J. X. Xu, Z. Q. Guo, and T. H. Lee, "Design and Implementation of Integral Sliding-Mode Control on an Underactuated Two-Wheeled Mobile Robot," IEEE Transactions on Industrial Electronics, vol. 61, no. 7, pp. 3671-3681, 2014, doi: 10.1109/TIE.2013.2282594.

[15] M. Cui, "Observer-Based Adaptive Tracking Control of Wheeled MobileRobots With Unknown Slipping Parameters," in IEEE Access, vol. 7, pp. 169646-169655, 2019.

[16] C. N. Savithri, R. S. Roopesh, N. Lavanya Devi, P. Shanthakumar, and P. Thirumurugan, "Self-balancing robot using arduino and PID controller," in Lecture Notes in Electrical Engineering,Singapore: Springer Nature Singapore, 2023, pp. 201–208, https://doi.org/10.1007/978-981-19-7169-3_18

[17] S. Kim and S. Kwon, "Dynamic modeling of a two-wheeled inverted pendulum balancing mobile robot," International Journal of Control, Automation and Systems, vol. 13, no. 4, pp. 926-933, 2015/08/01 2015, doi: 10.1007/s12555-014-0564-8.

[18] H. Pacejka and I. Besselink, Tire and Vehicle Dynamics. Elsevier Science, 2012.

[19] V. Utkin, "Variable structure systems with sliding modes," IEEE Transactions on Automatic Control, vol. 22, no. 2, pp. 212-222, 1977, doi: 10.1109/TAC.1977.1101446.

[20] H. K. Khalil, Nonlinear Systems. Prentice Hall, 2002.

[21] J.-J. E. Slotine and W. Li, Applied nonlinear control (no. 1). Prentice hall Englewood Cliffs, NJ, 1991.

[22] S. K. Y. Nikravesh, Nonlinear Systems Stability Analysis: Lyapunov-based Approach. CRC Press, 2013.

[23] A. Maddahi and A. H. Shamekhi, "Controller design for two-wheeled self-balancing vehicles using feedback linearisation technique," International Journal of Vehicle Systems Modelling and Testing, vol. 8, no. 1, pp. 38-54, 2013/01/01 2013, doi: 10.1504/IJVSMT.2013.052241.

[24] S. P. Bhattacharyya, A. Datta, and L. H. Keel, Linear Control Theory: Structure, Robustness, and Optimization. CRC Press, 2009.

[25] J. Villacrés, M. Viscaíno, M. Herrera, and O. Camacho, "Controllers Comparison to stabilize a Two-wheeled Inverted Pendulum: PID, LQR and Sliding Mode Control," International Journal of Control Systems and Robotics, vol. 1, pp. 29-36, 01/01 2016.

[26] Kruse, O., Mukhamejanova, A., Mercorelli, P., 2022. Super-twisting sliding mode control for differential steering system in vehicular yaw tracking motion. Electronics 11. 2022.

[27] O. Kruse et al. "Differential Steering System for Vehicular Yaw Tracking Motion with Help of Sliding Mode Control," 2022 23rd International Carpathian Control Conference (ICCC), Sinaia, Romania, 2022, pp. 58-63, doi: 10.1109/ICCC54292.2022.9805966